

Three-Dimensional Reconstruction of Maize Plants and Extraction of Phenotypic Parameters Based On Laser Point Cloud Data

Chengxin Ju (✉ cxju@yzu.edu.cn)

Yangzhou University <https://orcid.org/0000-0001-9457-9540>

Yuanyuan Zhao

Yangzhou University

Fengfeng Wu

Yangzhou University

Rui Li

Yangzhou University

Tianle Yang

Yangzhou University

Xiaochun Zhong

Ministry of Agriculture and Rural Affairs of the People's Republic of China

Feng Yan

Justus Liebig Universitat Giessen

Tao Liu

Yangzhou University <https://orcid.org/0000-0001-6788-1330>

Chengming Sun

Yangzhou University

Research Article

Keywords: laser point cloud, phenotypic parameters acquisition, three-dimensional reconstruction, point cloud processing

Posted Date: November 15th, 2021

DOI: <https://doi.org/10.21203/rs.3.rs-1037660/v1>

License:  This work is licensed under a Creative Commons Attribution 4.0 International License.

[Read Full License](#)

1 **Three-dimensional reconstruction of maize plants and**
2 **extraction of phenotypic parameters based on laser point**
3 **cloud data**

4 Chengxin Ju¹, Yuanyuan Zhao¹, Fengfeng Wu¹, Rui Li¹, Tianle Yang¹, Xiaochun
5 Zhong², Feng Yan³, Tao Liu^{1*}, Chengming Sun^{1*}

6 ¹Jiangsu Key Laboratory of Crop Genetics and Physiology/Co-Innovation Center for
7 Modern Production Technology of Grain Crops, Yangzhou University, Yangzhou
8 225009, China

9 ²Key Laboratory of Agricultural Information Services Technology, Ministry of
10 Agriculture and Rural Affairs, Beijing 100081, China

11 ³Department of Agronomy and Crop Physiology, Justus Liebig University Giessen,
12 Giessen D-35392, Germany

13 **E-mail**

14 Chengxin Ju: cxju@yzu.edu.cn; Yuanyuan Zhao: 1632594894@qq.com; Fengfeng Wu:
15 1756423192@qq.com; Rui Li: ruili023@163.com; Tianle Yang: 5997643@qq.com;
16 Xiaochun Zhong: Zhongxiaochun@caas.cn; Feng Yan: feng.yan@agrar.uni-giessen.de;
17 Tao Liu: 34626459@qq.com; Chengming Sun: cmsun@yzu.edu.cn.

18 * **Correspondence:** Corresponding Author

19 **Abstract**

20 **Background:** Three-dimensional (3D) laser scanning technology could rapidly extract
21 the surface geometric features of maize plants to achieve non-destructive monitoring of
22 maize phenotypes. However, extracting the phenotypic parameters of maize plants
23 based on laser point cloud data is challenging.

24 **Methods:** In this paper, a rotational scanning method was used to collect the data of
25 potted maize point cloud from different perspectives by using a laser scanner. Maize
26 point cloud data were grid-reconstructed and aligned based on greedy projection
27 triangulation algorithm and iterative closest point (ICP) algorithm, and the random
28 sampling consistency algorithm was used to segment the stem and leaf point clouds of
29 single maize plant to obtain the plant height and leaf parameters.

30 **Results:** The results showed that the R^2 between the predicted plant height and the
31 measured plant height was above 0.95, and the R^2 of the predicted leaf length, leaf width
32 and leaf area were 0.938, 0.878 and 0.956 respectively when compared with the
33 measured values.

34 **Conclusions:** The 3D reconstruction of maize plants using the laser scanner showed a
35 good performance, and the phenotypic parameters obtained based on the reconstructed
36 3D model had high accuracy. The results were helpful to the practical application of
37 plant 3D reconstruction and provided guidance for plant parameter acquisition and
38 theoretical methods for intelligent agricultural research.

39 **Keywords:** laser point cloud; phenotypic parameters acquisition; three-dimensional
40 reconstruction; point cloud processing

41

42 **Background**

43 Accurate and rapid acquisition of 3D plant structure information is important for high-
44 throughput phenotypic analysis, visualization and synergistic analysis of plant function
45 and structure [1-3]. With the development of agricultural intelligence, laser scanning
46 technology and its application in agriculture have become one of the hot spots for
47 research [4-6]. Compared with traditional measurement methods, laser technology
48 offers faster measurement, higher accuracy, and fuller digital features [7]. Su et al.
49 proposed a method to extract phenotypic information of maize plants in a field using
50 ground-based LiDAR [8]. Garrido et al. presented a new methodology for
51 georeferenced 3D reconstruction of maize plant structure [9]. There were still problems
52 such as low accuracy, expensive equipment and complicated operation in crop 3D
53 reconstruction research, most field phenotyping platforms could not obtain fine
54 phenotypic traits of single plant, and the recognition efficiency was determined to a
55 large extent by the shading between crops [10]. To obtain a complete 3D reconstruction
56 model of a single maize plant, a rotational scanning method was established in this
57 study, using potted maize as material, to provide a reference for 3D reconstruction and
58 phenotype acquisition of maize plants.

59 Phenotypic parameters such as plant height and leaf morphology are of great
60 importance in crop morphology studies [11-12]. 3D plant modeling provides a non-

61 destructive means to measure geometric properties and phenotypic parameters of crops
62 and allows studies at the individual organ level [13]. However, aspects such as stitching
63 and segmentation of 3D point cloud data are challenging, especially for maize in the
64 young stage when the young leaves are not yet fully expanded. Based on the above, this
65 paper acquired complete maize point cloud data by a portable laser scanner,
66 reconstructed and stitched the point clouds of single maize plant to obtain phenotypic
67 parameters such as plant height and geometric properties of leaves, then analyzed and
68 compared them with the measured values. The results of the study were suitable for the
69 3D reconstruction of plants with different degrees of complexity and could provide
70 references for 3D virtual simulation of maize and plant phenotype research.

71

72 **Methods**

73 **Experimental design**

74 During the maize growing season in 2019 and 2020, field experiments were conducted
75 at a research site at Yangzhou City, in the lower reaches of the Yangtze River, China
76 (32°39' N, 119°42' E). This is an alluvial plain and is one of the primary maize
77 production areas in China. The soil was a sandy loam with pH 6.88 [Typic Fluvaquents,
78 Etisols (U.S. taxonomy)]. The average values of soil properties of the field across the
79 study years were as follows: total N of 1.12g kg⁻¹, available phosphorus of 31.74 mg
80 kg⁻¹, available potassium of 74.43 mg kg⁻¹, organic matter of 23.57 g kg⁻¹, 1.34 g cm⁻³
81 of bulk density and 0.18 g g⁻¹ of field capacity. Climate data across the study years were
82 measured at a local weather station in the field site. The average precipitation, sunshine

83 hours, and mean air temperature that concerned the entire vegetation period were 125
84 mm, 193 h, and 25.2 °C in 2019, and 144 mm, 182 h, and 24.6 °C in 2020, respectively.
85 Three varieties Jingkenuo (VA), Huitian 8 (VB) and Zijiaoxi (VC) were used as the
86 research material. The plant height and leaf phenotypic parameters of the three varieties
87 differed significantly, with plant height gradually decreasing from VA to VC. Compared
88 with VA, the leaves of VB were relatively wide and long, and those of VC were
89 relatively narrow and short. Seeds of tested varieties were provided by Yangzhou Seed
90 Company (Yangzhou, China).

91 **Point cloud data acquisition**

92 The point cloud data was acquired using a rotational scanning method with a device
93 consisting of a computer system, scanner equipment and a rotating platform. The
94 scanner (Space Spider, Artec Corporation, Luxembourg) was fixed on a tripod, and the
95 maize plants were fixed on a rotating platform with a speed of 1-2 r/min, then the plants
96 were scanned at 360° using the scanner. The angle between the scanner lens and the
97 plant was in the range of 45° to 60°.

98 **Point cloud alignment and denoising**

99 Point cloud alignment was performed using the Iterative Closest Point (ICP) algorithm,
100 which found the corresponding point pair set between the two sets of point cloud data
101 and calculated the transformation matrix between them by iterating continuously to
102 obtain the matching relationship between the target and source point cloud sets. Each
103 truncated maize plant had two-point cloud outputs. The two acquired point clouds were

104 denoted as point cloud 1 and point cloud 2. The rotation and translation matrices R and
105 T to be solved by the ICP algorithm can be expressed as Eq:

$$\begin{bmatrix} X \\ Y \\ Z \end{bmatrix} = R \begin{bmatrix} X_i \\ Y_i \\ Z_i \end{bmatrix} + T \quad (1)$$

106 After obtaining the matrices R and T, the next step was to convert each point in
107 point cloud 2 with the current R and T, i.e. point cloud 2 and point cloud 1 to the same
108 3D coordinate system, thus completing the stitching process.

109 Point cloud denoising was performed using an irregular triangular network
110 encryption algorithm, which created a sparse irregular triangular network from seed
111 points, where the number of neighboring points ($K=5$) of all points within a user-
112 defined search radius $r=5$ mm, and if less than K neighboring points were found, one
113 point was removed as noise until all invalid points were identified and removed. This
114 method effectively reduced the number of noisy points without losing the true surface
115 points.

116 **Point cloud segmentation**

117 The stem and leaf point cloud of a single maize plant was segmented based on a random
118 sampling consistency (RANSAC) algorithm. The equations are shown below:

$$119 \quad (x - x_0)^2 + (y - y_0)^2 + (z - z_0)^2 = \frac{[l(x-x_0)^2 + m(y-y_0)^2 + n(z-z_0)^2]^2}{l^2 + m^2 + n^2} \quad (2)$$

120 where (x_0, y_0, z_0) was a point on the cylindrical axis, (l, m, n) was the direction
121 vector of the cylindrical axis.

122 **Plant parameters extraction**

123 Define the vertical distance from the junction of the base of the stem with
124 the soil to the highest point of the plant as the plant height, and:

$$125 \quad H = z_{max} - z_{min} \quad (3)$$

126 where z_{max} and z_{min} were the z-axis coordinates of the highest and lowest
127 points in the single plant point cloud, respectively.

128 The leaf length and width were the sums of the Euclidean distances between the
129 leaf skeleton points, and the leaf skeleton model was obtained by extracting the leaf
130 vein points with greater curvature in the triangular mesh model.

131 The maize blade was divided and firstly triangulated using the greedy projection
132 triangulation algorithm. The blade model after faceting was composed of several spatial
133 triangulation facets, then the area of a single spatial triangulation facet was calculated
134 through the Helen formula, and finally, the area of a single blade was calculated through
135 the area summation formula, which was calculated as follows:

$$136 \quad S_i = \sqrt{p_i(p_i - a_i)(p_i - b_i)(p_i - c_i)} \quad (4)$$

$$137 \quad S = \sum_{i=0}^n S_i \quad (5)$$

138 where: p_i was half the perimeter of the faceted triangle, a_i , b_i , c_i were the
139 lengths of the sides of the faceted triangle, n was the total number of facets, and i was
140 the facet index number.

141 **Plant parameter measurement**

142 The plant height was the shortest distance from the rootstock to the tip of all target
143 plants using a straightedge. The leaf length was the distance from the base of the leaf
144 to the tip of the leaf with a straightedge. The leaf width was the maximum width of the

145 leaf. The single leaf area was determined using the formula: leaf area = leaf length *
146 leaf width * 0.85. The total leaf area was the sum of the individual leaf areas of the
147 whole plant.

148 **Application of the data set**

149 Linear regression analysis was performed between manually measured data and data
150 extracted through the point cloud model. A scatter plot of 1:1 was created to test the
151 model fit. The independent data from Experiment 2020 was used to test the line
152 equations by comparing the differences in the estimation accuracy with the coefficient
153 of determination (R^2) and root mean square (RMSE). R^2 and RMSE were calculated
154 using Eqs. (6) and (7), respectively:

$$155 \quad R^2 = \frac{\sum_{i=1}^n (x_i - \bar{x})^2 \times (y_i - \bar{y})^2}{\sum_{i=1}^n (x_i - \bar{x})^2 \times \sum_{i=1}^n (y_i - \bar{y})^2} \quad (6)$$

$$156 \quad \text{RMSE} = \sqrt{\frac{\sum_{i=1}^n (y_i - x_i)^2}{n}} \quad (7)$$

157 where x_i , \bar{x} , y_i , \bar{y} were the measured value, the mean of measured values, the
158 predicted value, and the mean of predicted values, respectively, n was the number of
159 measurements.

160 **Results and analysis**

161 **Crop 3D reconstruction based on point cloud data**

162 *Point cloud triangulation*

163 The results shown in Fig. 1 (b, d) were based on the greedy projection triangulation
164 algorithm to reconstruct the point cloud data on a grid. The results showed that the
165 algorithm used could effectively complete the grid reconstruction of the plant point

166 cloud data, and lead to good reconstruction results.

167 ***Point cloud splicing***

168 Due to the great height of the maize plants after the elongation stage, it was difficult to
169 use the laser scanner to acquire all the plant point cloud data at once, so the plants
170 needed to be truncated and acquired segmented, and then the segmented point clouds
171 needed to be spliced together. Fig. 2 showed the splicing effect of the 3D point cloud
172 splicing of truncated maize plants. As the figure showed, the point clouds obtained
173 under the rotating platform were completely spliced of the maize plants. Since the three
174 varieties exhibited a similar splicing effect, that of VB was only presented for
175 conciseness.

176 ***Point cloud segmentation***

177 Fig. 3 showed the 3D point cloud and plant conformation segmentation results of maize
178 plants, where individual leaf skeletons are visualized with random colors. The leaf
179 visualization of the 3D model represented a maize leaf *in vivo*, and the segmentation
180 results of individual leaves matched well with the maize plants in real growth conditions.
181 The results showed that the organ segmentation method used in this study could
182 effectively extract each leaf from the 3D point cloud of the maize plant.

183 ***Plant leaf midrib fitting***

184 The stems were extracted according to the random sampling consistency algorithm
185 mentioned above, and then each leaf was separated by using the Euclidean clustering
186 algorithm. This fitting was done with three different maize varieties (VA, VB, and VC).

187 Fig. 4 showed the dense point cloud (a-c), skeleton (d-f), and leaf midrib (g-i) of the

188 reconstructed maize plants at the growth stage of 35 days after seedling emergence.
189 Leaf midrib of different leaves was represented by different colors, and the leaf blade
190 midrib was accurately fitted by using the method of this study.

191 **Phenotype parameter extraction and accuracy analysis**

192 *Plant height extraction and accuracy analysis*

193 The model accuracy was verified by comparing the predicted plant height extracted by
194 the model and the measured plant height. As shown in Fig. 5, there was a good
195 correlation between the predicted and measured values, and for all three varieties R^2
196 was greater than 0.95. The R^2 and RMSE were 0.969 and 2.718 cm for VA, 0.954 and
197 2.994 cm for VB, and 0.967 and 2.732 cm for VC, respectively. The R^2 and RMSE
198 were 0.964 and 2.818 cm for three varieties together. This indicates that the method
199 used in the present study could represent the plant height *in vivo*. Since the method was
200 not sensitive to varieties, the leaf phenotypic parameters were no longer analyzed
201 separately for varieties.

202 *Extraction and accuracy analysis of leaf phenotypic parameters*

203 Taking a maize plant 25 days after emergence as an example, and at this time, all six
204 spreading leaves of the plant were visible. As shown in Fig. 6, the predicted and
205 observed values of leaf length, leaf width and leaf area showed highly significant
206 positive correlations. The average R^2 and RMSE of tested varieties were 0.938 and
207 2.596 cm of leaf length, 0.878 and 0.273 cm of leaf width, and 0.956 and 4.494 cm² of
208 leaf area respectively. Although the edge of the leaf is poorly reconstructed in the
209 process due to the long and slender leaf tip of maize leaves, it could still provide a

210 reference for obtaining phenotypic parameters based on the point that could reconstruct
211 plants.

212 **Discussion**

213 With the development of 3D scanning equipment and 3D reconstruction technology,
214 3D scanning technology finds a wide range of applications in various aspects of
215 agricultural production research, especially in crop 3D reconstruction and phenotype
216 research [14]. Reik *et al.* developed a multi-scale method using airborne laser scanning
217 data with point densities to determine the number and vertical extent of canopy layers
218 [15]. Gaillard *et al.* used a laser scanner combined with a movable measuring arm to
219 acquire 3D point cloud data of barley to achieve organ-specific growth monitoring of
220 barley plants [16]. Tsoulas *et al.* mounted a laser scanning system on a tractor to obtain
221 the 3D structural parameters of apple trees [17]. Chang *et al.* developed a method for
222 detecting sorghum spikes using unmanned aerial vehicle (UAV) images to extract 3D
223 point clouds, and the results showed that the correlation coefficients between the spike
224 length and width measured by the UAV and those measured on the ground were 0.61
225 and 0.83, respectively [18]. In the above-mentioned studies, either the accuracy of the
226 data obtained was not high or the equipment was too expensive for most researchers to
227 afford. These studies were suitable for high throughput acquisition of phenotypic data
228 under field conditions. However, for some indoor experiments requiring higher
229 precision analysis of phenotypic properties, particularly in plant breeding programs, the
230 present study provided a feasible solution. Field maize or other crops could also be
231 reconstructed by the method established in this study.

232 Although the 3D reconstruction of plants based on laser scanning data had high
233 accuracy, there were still many drawbacks due to the movement of instruments and
234 human factors during the scanning process, and the use of laser scanners to obtain high-
235 precision 3D models of plants required obtaining point cloud data from different angles
236 [19-20]. When performing point cloud data acquisition, plant shaking during
237 acquisition due to the exposure of the scanner's lens exposure or the rotation of the
238 turntable could cause the loss of point cloud data, resulting in the degradation of the
239 quality of the grid generated later [21]. In the present study, the lens was fixed to avoid
240 the loss of accuracy caused by the movement of the lens, and the platform rotated slowly
241 to ensure the integrity and accuracy of the point cloud acquisition.

242 In this paper, we achieved 3D reconstruction of maize plants through the processes
243 of point cloud data acquisition, alignment, denoising, and segmentation. In addition to
244 the point cloud information, we also obtained information on the color and texture of
245 the plants, which could be very useful for analysis of plant properties related to crop
246 nutrition, disease or yield, which will be focused on in the future. The collection of
247 plant point cloud data using laser scanners were insufficient in the large-scale
248 automated measurement of phenotypic information, so the studies of algorithms for
249 automated acquisition of phenotypic information were one of the next steps. This could
250 be done by means such as adding a robotic arm, or by proposing a deep learning
251 framework to acquire object point cloud data from multi-view images for 3D
252 reconstruction, which in turn improved the reconstruction efficiency [16, 22].

253 The 3D model of maize plants obtained from laser point cloud 3D reconstruction

254 had a high reconstruction accuracy and could describe the plant structure and
255 characteristics in detail, meeting the requirements for accurate measurement of plant
256 phenotypic data. In this study, the correlation coefficients between the predicted values
257 and observed values of plant height, leaf length and leaf area were above 0.93, and the
258 correlation coefficient of leaf width reached 0.87 (Fig. 5 and 6). Compared with the
259 conventional leaf area measurement method (length times width times factor), the leaf
260 area measured in this study has theoretically higher accuracy and no damage to the plant.
261 In addition, it was convenient to collect point cloud data by a laser scanner, but the
262 subsequent processing consumed some time. With the development of graphics
263 processing unit computing, the post-processing time was greatly reduced, but it still
264 could not meet the need for real-time reconstruction. With the rapid development of
265 simultaneous localization and mapping technology, a more efficient reconstruction
266 algorithm would become a hot spot for future research.

267 **Conclusion**

268 We proposed a 3D reconstruction method for maize plants based on laser point cloud
269 data, which effectively reconstructed the detailed features of the plants and accurately
270 reflected the plant morphology. Through the iterative closest point algorithm and the
271 random sampling consistency algorithm, the point cloud data were aligned and
272 segmented to further improve the maize 3D reconstruction model. The plant parameters
273 obtained by the reconstructed model showed high consistency with the observed values,
274 which could provide a reference for obtaining phenotypic parameters based on the
275 reconstructed plants.

276 **Acknowledgments**

277 Not applicable for that section.

278 **Authors' contributions**

279 Conceptualization, CJ and CS; methodology, TL and XZ; software, FW and TY; formal
280 analysis, YZ and RL; data curation, YZ and TY; writing—original draft preparation,
281 FW and RL. writing— review and editing, CJ and FY. All authors were involved in
282 preparing and revising the manuscript.

283 **Funding**

284 This research was financially supported by the National Natural Science Foundation of
285 China (32172110, 32001465, 31872852), the National Key Research and Development
286 Program of China (2018YFD0300805), the Key Research and Development Program
287 (Modern Agriculture) of Jiangsu Province (BE2020319), and the Priority Academic
288 Program Development of Jiangsu Higher Education Institutions (PAPD).

289 **Availability of data and material**

290 All data analyzed during this study are presented in this published article.

291

292 **Declarations**

293 **Ethics approval and consent to participate**

294 Not applicable for that section.

295 **Consent for publication**

296 All authors have seen the manuscript and approved to submit to your journal. All
297 authors agree to publish.

298 **Competing interests**

299 The authors declare that they have no competing interests.

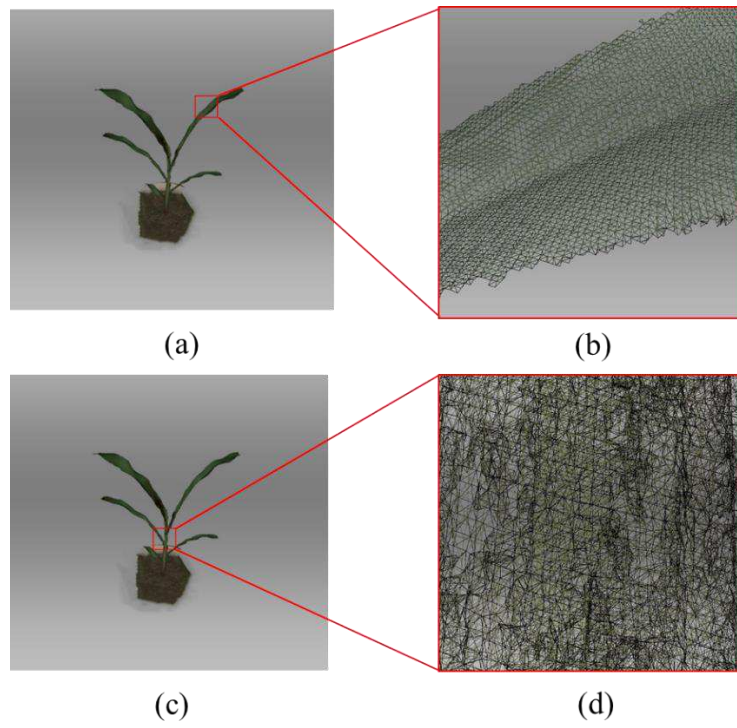
300 **Author details**

301 ¹Jiangsu Key Laboratory of Crop Genetics and Physiology/Co-Innovation Center for
302 Modern Production Technology of Grain Crops, Yangzhou University, Yangzhou
303 225009, China. ²Key Laboratory of Agricultural Information Services Technology,
304 Ministry of Agriculture and Rural Affairs, Beijing 100081, China. ³Department of
305 Agronomy and Crop Physiology, Justus Liebig University Giessen, Giessen D-35392,
306 Germany.

307 **References**

- 308 1. Junker A, Muraya MM, Weigelt-Fischer K, et al. Arana-Ceballos F, Klukas C, Melchinger AE,
309 Meyer RC, Riewe D, Altmann T. Optimizing experimental procedures for quantitative
310 evaluation of crop plant performance in high throughput phenotyping systems. *Front Plant Sci.*
311 2015; 5: 143–152.
- 312 2. Zhang XH, Huang CL, Wu D, Qiao F, Li WQ, Duan LF, Wang K, Xiao YJ, Chen GX, Liu Q,
313 Xiong LZ, Yang WN. High-throughput phenotyping and QTL mapping reveals the genetic
314 architecture of maize plant growth. *Plant Physiol.* 2017; 173: 1554–1564.
- 315 3. Thapa S, Zhu FY, Walia H, Yu HF, Ge YF. A Novel LiDAR-Based Instrument for High-
316 Throughput, 3D Measurement of Morphological Traits in Maize and Sorghum. *Sensors-Basel.*
317 2018; 18: 1187–1196.
- 318 4. Du JJ, Zhang Y, Guo XY, Ma LM, Shao M, Pan XD, Zhao CJ. Micron-scale phenotyping
319 quantification and three-dimensional microstructure reconstruction of vascular bundles within
320 maize stalks based on micro-CT scanning. *Funct Plant Biol.* 2016; 44: 10–22.
- 321 5. Liu SY, Baret F, Abichou M, Boudon F, Thomas S, Zhao KG, Fournier C, Andrieu B, Irfan K,
322 Hemmerlé M, Solan B. Estimating wheat green area index from ground-based LiDAR
323 measurement using a 3D canopy structure model. *Agr Forest Meteorol.* 2017; 247: 12–20.
- 324 6. Vázquez-Arellano M, Reiser D, Paraforos DS, Garrido-Izard M, Burce MEC, Griepentrog HW.
325 3-D reconstruction of maize plants using a time-of-flight camera. *Comput Electron Agr.* 2018;
326 14: 235–247.
- 327 7. Guan XP, Liu K, Qiu BJ, Dong XY, Xue XY. Extraction of geometric parameters of soybean
328 canopy by airborne 3D laser scanning. *Trans CSAE.* 2019; 35: 96–103.
- 329 8. Su W, Jiang KP, Guo H, Liu Z, Zhu DH, Zhang JD. Extraction of phenotypic information of
330 maize plants in field by terrestrial laser scanning. *TransCSAE.* 2019; 35: 125–130.
- 331 9. Garrido M, Paraforos DS, Reiser D, Vázquez-Arellano M, Griepentrog HW, Valero C. 3D
332 maize plant reconstruction based on georeferenced overlapping LiDAR point clouds. *Remote*

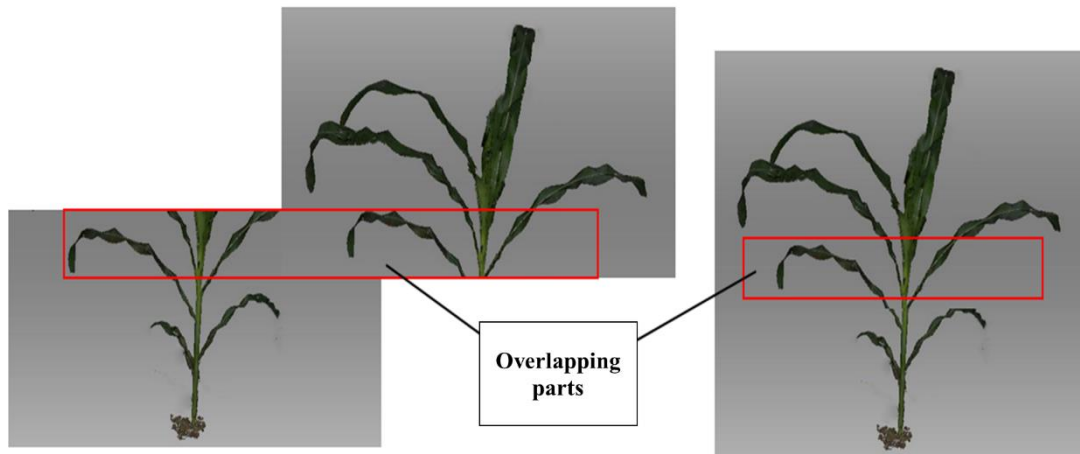
- 333 Sens-Basel. 2015; 7: 17077–17096.
- 334 10. Young SN, Kayacan E, Peschel JM. Design and field evaluation of a ground robot for high-
335 throughput phenotyping of energy sorghum. *Precis Agric.* 2019; 20: 697–722.
- 336 11. Sun SP, Li CY, Paterson AH. In-field high-throughput phenotyping of cotton plant height using
337 LiDAR. *Remote Sens-Basel.* 2017; 9: 377.
- 338 12. Virlet N, Sabermanesh K, Sadeghitehran P, Hawkesford MJ. Field Scanalyzer: An automated
339 robotic field phenotyping platform for detailed crop monitoring. *Funct Plant Biol.* 2016; 44:
340 143–153.
- 341 13. Sritarapipat T, Rakwatin P, Kasetkasem T. Automatic Rice Crop Height Measurement Using a
342 Field Server and Digital Image Processing. *Sensors-Basel.* 2014; 14: 900–926.
- 343 14. Mattei E, Castrodad A. Point Cloud Denoising via Moving RPCA. *Comput Graph Forum.* 2017;
344 36: 123–127.
- 345 15. Reik L, Hossein T, Reinhard F, Michael S, Felix M. Towards Automated Characterization of
346 Canopy Layering in Mixed Temperate Forests Using Airborne Laser Scanning. *Forests.* 2015;
347 6: 4146–4167.
- 348 16. Gaillard M, Miao CY, Schnable J, Benes B. Sorghum segmentation by skeleton extraction.
349 *Lect Notes Comput Sci.* 2020; 28: 296–311.
- 350 17. Tsoulas N, Paraforos DS, Fountas S, Zude-sasse M. Estimating canopy parameters based on
351 the stem position in apple trees using a 2D LiDAR. *Agronomy-Basel.* 2019; 9: 740–758.
- 352 18. Chang A, Jung J, Yeom J, Landivar J. 3D characterization of sorghum panicles using a 3D point
353 cloud derived from UAV imagery. *Remote sens-Basel.* 2021; 13: 282.
- 354 19. Wang YY, Wen ZL, Guo XY, Zhao GH, Lu SL, Xiao BX. Research on three-dimensional
355 reconstruction and visualization of above-ground tobacco plant. *Sci Agric Sin.* 2013; 46: 37–
356 44.
- 357 20. Guan XP, Chen YT, Zhang HQ, Liu M, Li YL. Method on tree point could model de-noising
358 based on bilateral filtering. *J Cent South Uni Forest Technol.* 2015; 35: 83–87.
- 359 21. Wu FF. Three-dimensional reconstruction and accuracy analysis of maize plants based on laser
360 scanning data. Master Thesis, Yangzhou University, Yangzhou, China, 2021.
- 361 22. Sharma S, Kumar V. Voxel-based 3D face reconstruction and its application to face recognition
362 using sequential deep learning. *Multimed Tools and Appl.* 2020; 79:17303–17330.
- 363
- 364



366
367
368

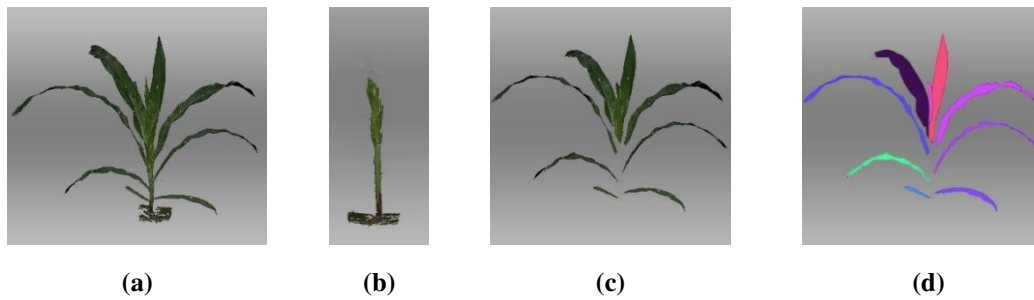
Fig. 1 Leaf (a-b) and stem (c-d) mesh effect based on greedy projection triangulation algorithm

369
370



371
372
373
374
375
376
377

Fig.2 Reconstruction of point cloud splicing of truncated maize plants

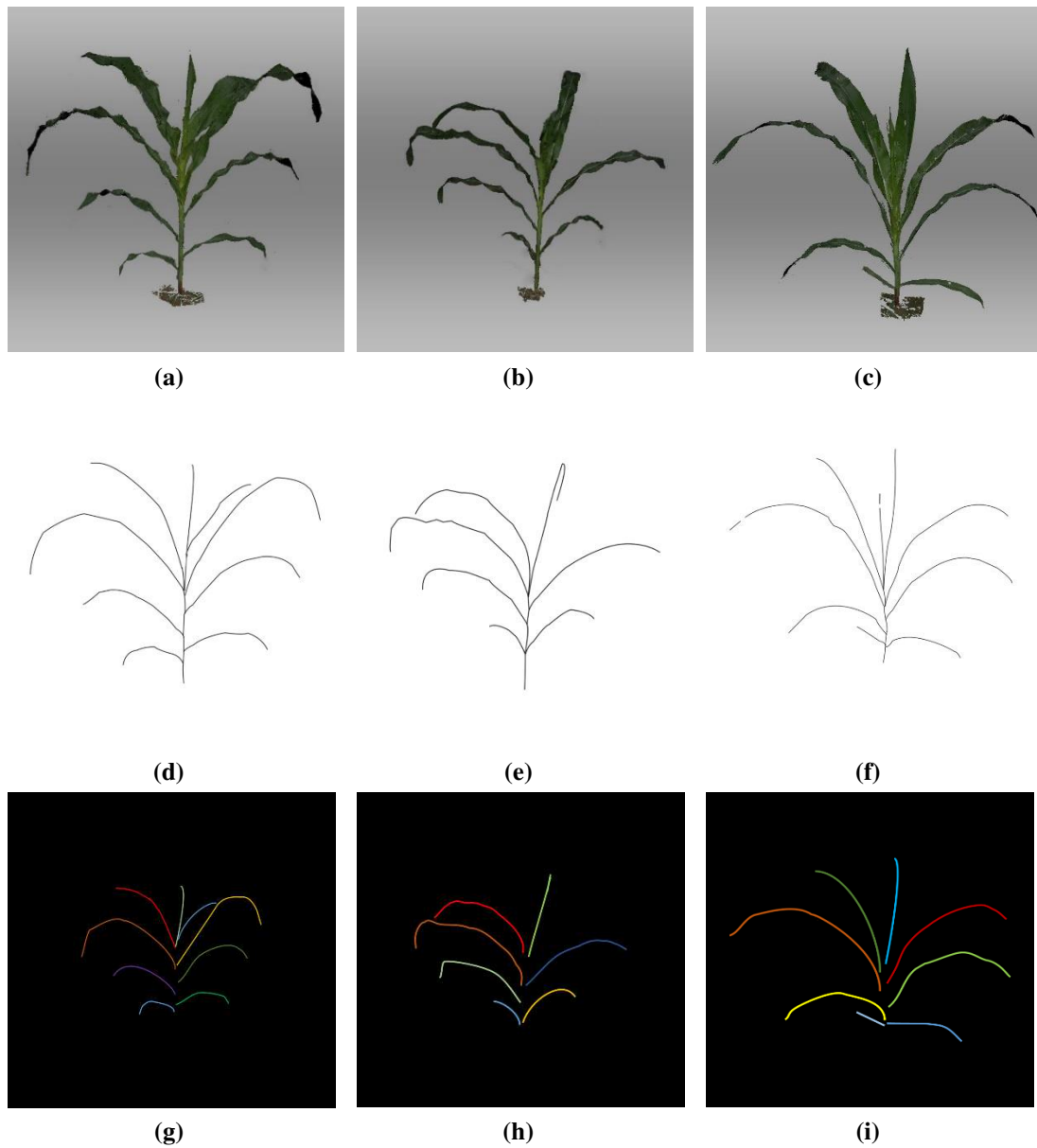


378
379
380
381

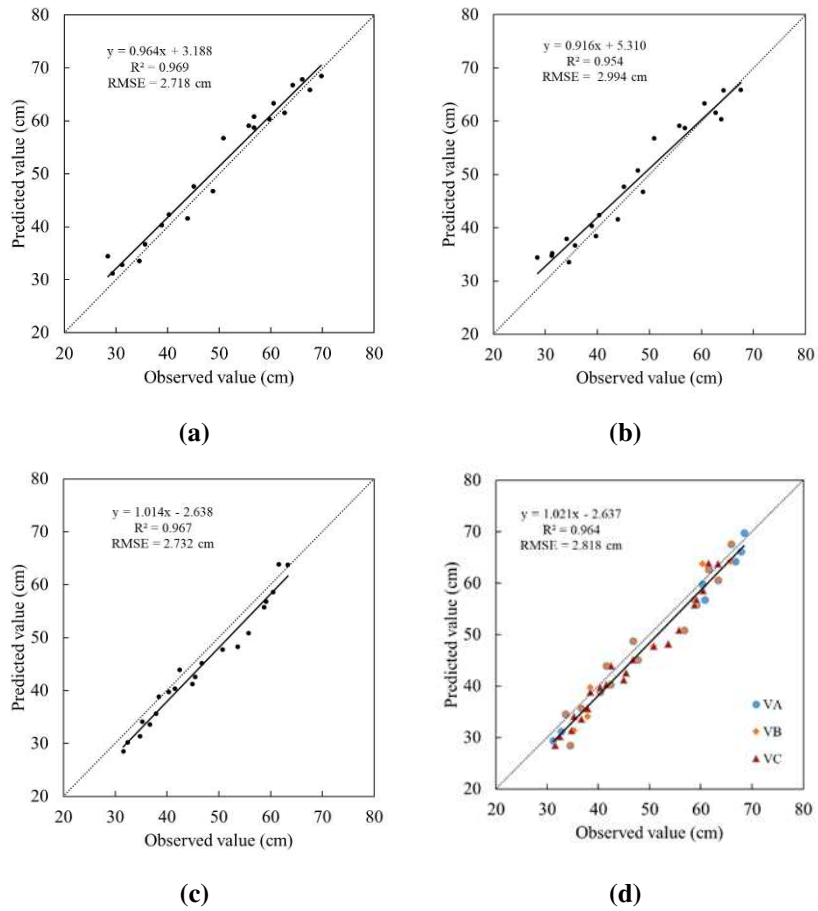
Fig. 3 Maize three-dimensional point cloud segmentation

(a) Maize plant point cloud, (b) Stem point cloud, (c) Leaf point cloud, (d) Single leaf point cloud

382
383



384 Fig. 4 Dense point cloud (a-c), skeleton (d-f), and leaf midrib (g-i) of maize plants
385 (a, d, g) VA, (b, e, h) VB, (c, f, i) VC
386



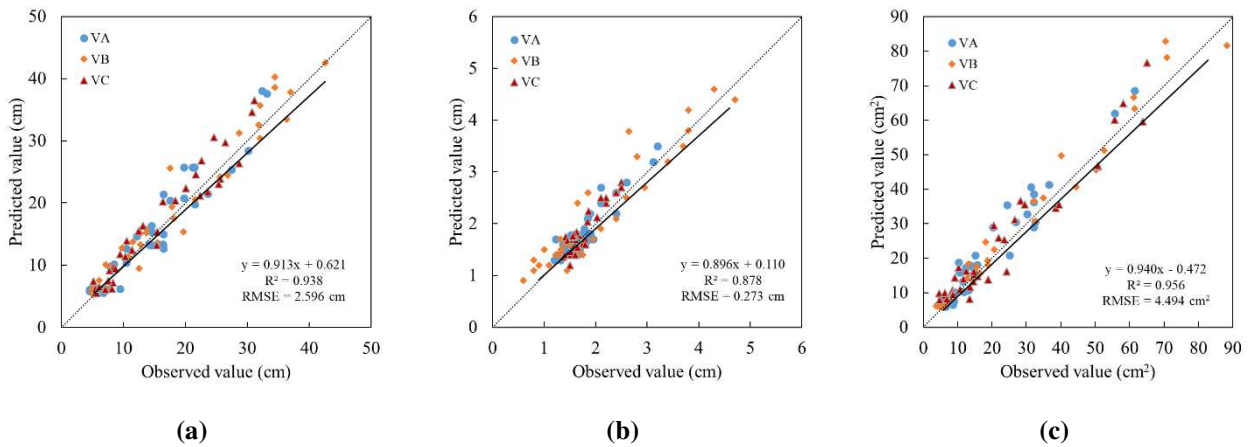
389 Fig. 5 Precision analysis of maize plant height of VA (a), VB (b), VC (c) and three maize
390 varieties (d)

391

392

393

394



395 Fig.6 Analysis on the precision of phenotypic parameters of leaf length (a), leaf width (b) and leaf
396 area (c) of three maize varieties

397